







Immune Imprinting Drives Human Norovirus Potential for Global Spread

 Lisa C. Lindesmith,^a Florencia A. T. Boshier,^b Paul D. Brewer-Jensen,^a Sunando Roy,^b Veronica Costantini,^c Michael L. Mallory,^a Mark Zweigart,^a Samantha R. May,^a Helen Conrad,^a Kathleen M. O'Reilly,^d Daniel Kelly,^e Cristina C. Celma,^f Stuart Beard,^f Rachel Williams,^{b,g} Helena J. Tutill,^g Sylvia Becker Dreps,^{a,h} Filemón Bucardo,ⁱ  David J. Allen,^e Jan Vinjé,^c  Richard A. Goldstein,^j Judith Breuer,^{b,k}  Ralph S. Baric^a

^aDepartment of Epidemiology, University of North Carolina, Chapel Hill, North Carolina, USA

^bDepartment of Infection, Immunity and Inflammation, UCL Great Ormond Street Institute of Child Health, University College London, London, United Kingdom

^cDivision of Viral Diseases, Centers for Disease Control and Prevention, Atlanta, Georgia, USA

^dCentre for Mathematical Modelling of Infectious Diseases, Department of Infectious Disease Epidemiology, London School of Hygiene and Tropical Medicine, London, United Kingdom

^eDepartment of Infection Biology, Faculty of Infectious and Tropical Diseases, London School of Hygiene and Tropical Medicine, London, United Kingdom

^fEnteric Virus Unit, The Virus Reference Department, UK Health Security Agency, London, United Kingdom

^gDepartment of Genetics & Genomic Medicine, UCL Great Ormond Street Institute of Child Health, University College London, London, United Kingdom

^hDepartment of Family Medicine, University of North Carolina at Chapel Hill, Chapel Hill, North Carolina, USA

ⁱDepartment of Microbiology, National Autonomous University of Nicaragua, León, León, Nicaragua

^jDivision of Infection and Immunity, University College London, London, United Kingdom

^kDepartment of Microbiology, Great Ormond Street Hospital for Children NHS Foundation Trust, London, United Kingdom

Lisa C. Lindesmith and Florencia A. T. Boshier contributed equally. This work combined two independently initiated studies. The author order was determined based on the order of completion of these initial studies.

Richard A. Goldstein, Judith Breuer, and Ralph S. Baric contributed equally.

ABSTRACT Understanding the complex interactions between virus and host that drive new strain evolution is key to predicting the emergence potential of variants and informing vaccine development. Under our hypothesis, future dominant human norovirus GII.4 variants with critical antigenic properties that allow them to spread are currently circulating undetected, having diverged years earlier. Through large-scale sequencing of GII.4 surveillance samples, we identified two variants with extensive divergence within domains that mediate neutralizing antibody binding. Subsequent serological characterization of these strains using temporally resolved adult and child sera suggests that neither candidate could spread globally in adults with multiple GII.4 exposures, yet young children with minimal GII.4 exposure appear susceptible. Antigenic cartography of surveillance and outbreak sera indicates that continued population exposure to GII.4 Sydney 2012 and antigenically related variants over a 6-year period resulted in a broadening of immunity to heterogeneous GII.4 variants, including those identified here. We show that the strongest antibody responses in adults exposed to GII.4 Sydney 2012 are directed to previously circulating GII.4 viruses. Our data suggest that the broadening of antibody responses compromises establishment of strong GII.4 Sydney 2012 immunity, thereby allowing the continued persistence of GII.4 Sydney 2012 and modulating the cycle of norovirus GII.4 variant replacement. Our results indicate a cycle of norovirus GII.4 variant replacement dependent upon population immunity. Young children are susceptible to divergent variants; therefore, emergence of these strains worldwide is driven proximally by changes in adult serological immunity and distally by viral evolution that confers fitness in the context of immunity.

IMPORTANCE In our model, preepidemic human norovirus variants harbor genetic diversification that translates into novel antigenic features without compromising viral fitness. Through surveillance, we identified two viruses fitting this profile, forming

Invited Editor Swati Jain, Catholic University of America

Editor Marthandan Mahalingam, Catholic University of America

Copyright © 2022 Lindesmith et al. This is an open-access article distributed under the terms of the [Creative Commons Attribution 4.0 International license](https://creativecommons.org/licenses/by/4.0/).

Address correspondence to Lisa C. Lindesmith, lisal@unc.edu, Ralph S. Baric, rbaric@email.unc.edu, Richard A. Goldstein, r.goldstein@ucl.ac.uk, or Judith Breuer, j.breuer@ucl.ac.uk.

The authors declare a conflict of interest. L.C.L. and R.S.B. hold patents on norovirus vaccine design and ongoing collaborations with VaxArt, Takeda Vaccines and HilleVax that are unrelated and do not pose conflicts of interest with this report. R.S.B. is a member of the advisory committee for VaxArt and Adagio Therapeutics. S.B.D. received an investigator-initiated research award from Takeda Vaccines unrelated to this report. P.B.J., M.L.M., M.R.Z., H.C., S.R.M., F.A.T.B., R.S., H.T., R.W., R.G., J.B., D.J.A., D.K., K.O., F.B., J.V., V.C., C.C.C., and S.B. have no conflicts of interest.

Received 1 July 2022

Accepted 25 August 2022

Published 14 September 2022

long branches on a phylogenetic tree. Neither evades current adult immunity, yet young children are likely susceptible. By comparing serological responses, we demonstrate that population immunity varies by age/exposure, impacting predicted susceptibility to variants. Repeat exposure to antigenically similar variants broadens antibody responses, providing immunological coverage of diverse variants but compromising response to the infecting variant, allowing continued circulation. These data indicate norovirus GII.4 variant replacement is driven distally by virus evolution and proximally by immunity in adults.

KEYWORDS norovirus, neutralizing antibodies, surveillance, epidemic, histo-blood group antigens, antigenic cartography, variants of concern, antigenic seniority, immune imprinting, sequencing, variant persistence

Human norovirus is the causative agent of ~20% of all acute gastroenteritis episodes worldwide (1). Although all age groups are infected, the most significant impact of disease is among young children and the elderly, who together bear the highest mortality rates, estimated at more than 200,000 deaths/year (2). This global disease burden has motivated the development of norovirus vaccines, with two candidates currently in clinical trials (3–5). Vaccine development is hampered by extensive diversity within the >35 known norovirus genotypes that infect humans (6). Recent progress in identifying key correlates of protection such as histo-blood group antigen (HBGA)-blocking antibodies (Ab) and the development of cell culture systems for several norovirus strains has accelerated vaccine development. Antigenic diversity within the GII.4 genotype, serotype/epitope-level cross-immunity, lack of understanding of the drivers of strain emergence, and the absence of a robust small animal model remain significant hurdles. Of these, antigenic diversity within the GII.4 genotype is the most significant obstacle to vaccine development (7–9). Norovirus global resurgence events occur cyclically and correspond with emergence of novel GII.4 variants characterized by unique constellations of residues within neutralizing antibody epitopes encoded within the capsid protein (VP1) (7, 9–11). Virus recombination between the genes that encode the RNA-dependent RNA polymerase (ORF1-NS7) and viral capsid (ORF2) types may also contribute to variant circulation and persistence in human populations (12–14).

Phylotemporal analysis of norovirus sequences suggests that preemergent GII.4 viruses with novel epitopes critical to immune escape circulate at endemic levels before becoming dominant, specifically in young children with limited GII.4 cross-protective immunity (15–17). Prior to global spread, these preemergent viruses would appear on phylogenetic trees at the end of atypically long branches. Population immunity would then determine which variants would successfully emerge and become dominant. As the most frequent cause of viral acute gastroenteritis outbreaks in the 21st century, six GII.4 norovirus variants have predominated worldwide in the past 25 years (18–20), resulting in significant burdens on health care, education, and military units (21–23). The first GII.4 variant with worldwide distribution emerged in the mid-1990s, followed by subsequent variant replacements in 2002 (circulation 2002 to 2005), 2004 (2004 to 2008), 2006 (2006 to 2011), 2009 (2009 to 2012), and 2012 (2012 to at least 2022). Notably, GII.4 Sydney 2012 viruses have not yet been replaced and continue to circulate globally and account for ~50% of norovirus outbreaks 10 years postemergence (24). Why this variant has persisted in the population for a decade is a fundamental question the field has yet to answer.

Here, based on preemergence diversification, we identified two candidate viruses fitting the phylogenetic characteristics of preepidemic variants and evaluated their emergence potential by comparing their susceptibilities to neutralization by sera from children and adults. Sera from young children were largely variant specific across time, whereas neutralization potency of sera from adults was broader with evidence of back-boosting to previously dominant GII.4 variants. These data support the idea that Sydney 2012 persistence may be driven by a lack of durable Sydney 2012-specific

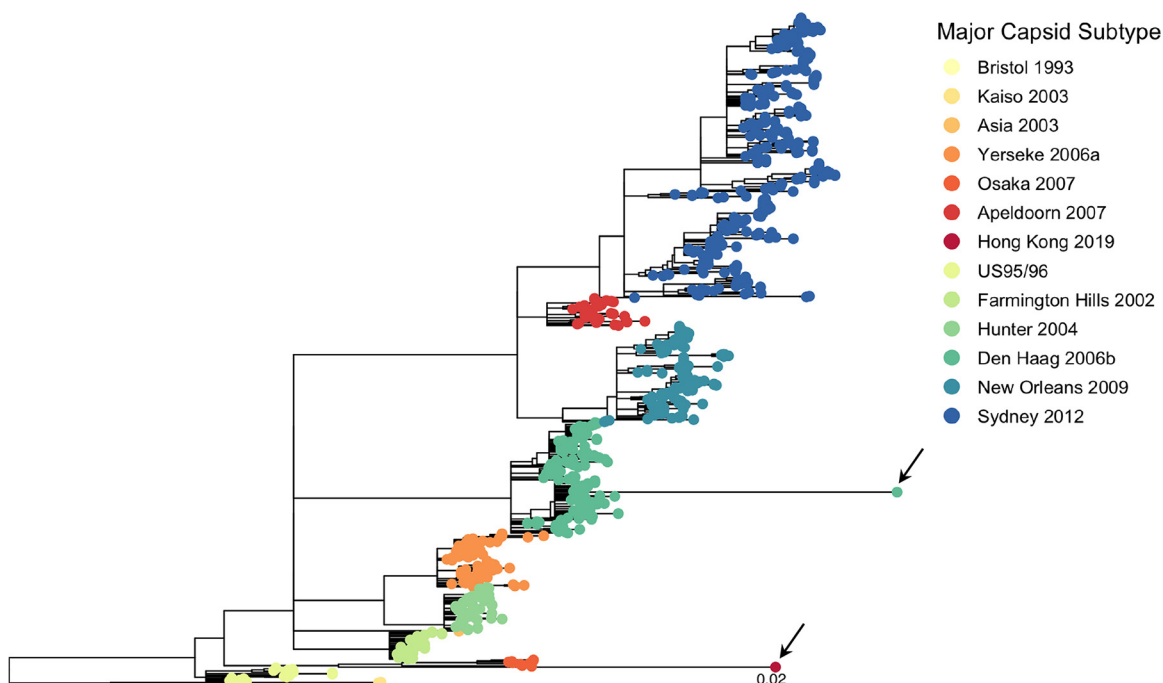


FIG 1 Maximum likelihood tree of 930 GII.4 major capsids generated by RAxML (66). Nodes with bootstrap support of less than 70 were collapsed. Rooting was optimized by TempEst (67). Tip color indicates major capsid subtype with epidemics in red tones and GII.4 viruses that spread globally in blue tones. Two long branches are observed: one leading to Hong Kong 2019 detected on 18 March 2019 and one leading to Den Haag 2017 detected on 21 February 2017. The corresponding tips are indicated by an arrow.

protective immunity in adults. Further, we found that continued exposure to GII.4 Sydney 2012 and antigenically related viruses results in a broadening of the immune response to include viruses characterized as potentially preemergent by phylogenetic analyses, potentially limiting new variant emergence. Consequently, we propose a model in which emerging variant selection is likely dependent upon the dynamics of the serological repertoire of adult populations with preexisting immunity, shaped and then reshaped by sequential GII.4 exposures (15, 25, 26).

RESULTS

Identification of highly divergent GII.4 variants by capsid gene sequence. To search for viruses with preemergent signatures, we analyzed 930 GII.4 norovirus ORF2 sequences from samples collected in the United Kingdom between 1994 and 2019; all possessed full complementary metadata (including age, gender, geography, and date of sample). Two taxa with atypically long branches were observed in the phylogenetic tree (Fig. 1; see also Fig. S1 in the supplemental material). The first, GII.4 Hong Kong 2019, demonstrated a rate of evolution in accordance with the remainder of the data (Fig. S2). It is most closely related to the GII.4 Osaka 2007 variant, although it diverged from this lineage well before the Osaka 2007 epidemic, in keeping with characteristics observed in known preepidemic variants (15) (Fig. S3). The second, GII.4 Den Haag 2017, emerged from within the GII.4 Den Haag 2006 cluster (Fig. S3).

Den Haag 2017 exhibits few changes in characterized antigenic regions (Fig. S4). It has 5 unique residues (294P, 339R, 340S, 378R, and 413A) relative to the 155 Den Haag 2006 strains in our data set; however, only 378R in antigenic site C is unique relative to all other strains in our data set. In contrast, Hong Kong 2019 possesses 16 unique antigenic site residues relative to the 10 Osaka 2007 strains in our data set (Fig. S4). Of these, six in antigenic sites A (298Q), D (393E, 395P, and 397F), and G (355A and 364N) are unique relative to all other strains in our data set. Unique combinations of residues in these sites are known to correlate with immune escape and widespread GII.4 variant emergence. Monitoring changes at known antigenic sites alone is insufficient to

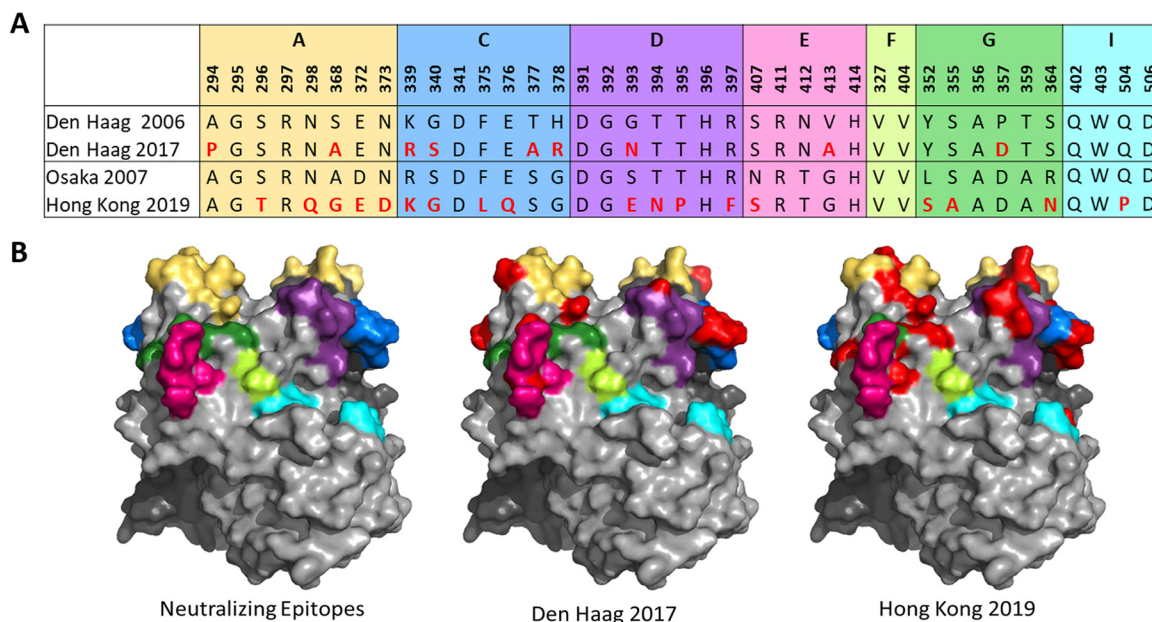


FIG 2 Sequence of GII.4 blockade/neutralizing antibody antigenic sites in divergent strains compared to those in closely related strains tested here. (A) Comparison of amino acid sequences in VP1 blockade/neutralizing antibody antigenic sites in Den Haag 2017 and Hong Kong 2019 to those in Den Haag 2006 and Osaka 2007 strains studied here as VLPs. (B) Blockade/neutralizing antibody antigenic sites mapped onto the surface of Sydney 2012 P domain dimer (PDB 4wzt). Residues differing between Den Haag 2017 and 2006 or Hong Kong 2019 and Osaka 2007 are colored red in both panels A and B. Complete capsid sequences for Den Haag 2019 and Hong Kong 2019 compared to their closest sequence neighbors are shown in Fig. S5.

predict strain emergence. Indeed, multiple GII.4 variants with differences within known neutralizing/blockade Ab antigenic sites have been shown to cocirculate (15), yet only six became predominant and spread globally (18–20). Thus, we developed a phenotype-based testing pipeline to evaluate the impact of genotype changes. All GII.4 variants that have spread globally share two features: novel neutralizing/ligand binding blockade antibody antigenic site profiles and binding to multiple cellular ligands (8, 20, 27, 28). Human noroviruses use ABO histo-blood group antigens (HBGAs) as cellular binding ligands (29, 30). HBGA expression varies between and within human populations; thus, the ability to bind to a diverse set of ligands corresponds to a potentially large susceptible population. The HBGA ligand binding pocket that binds the common glycan among ABO antigens is highly conserved across GII.4 variants; however, variation within residues 391 to 397 (antigenic site D) provides stabilizing interactions with ligands that impact variant avidity for different ABO HBGA as well as neutralizing antibodies (7, 8, 31–34). Den Haag 2017 and Hong Kong 2019 have substitutions within antigenic site D (Fig. 2). To investigate the phenotypic effect of these sequence changes on strain ligand binding, we developed representative virus-like particles (VLPs) for Den Haag 2017 and Hong Kong 2019 and matched ancestral strains of Den Haag 2006 and Osaka 2007 variants (Fig. 2).

Evaluation of divergent variant emergence potential based on capsid ligand binding profiles. Den Haag 2006, Osaka 2007, and Hong Kong 2019 displayed robust binding to native ligands in porcine gastric mucin (PGM) which includes H, A, and Lewis Y antigens and to human blood group B saliva (B antigen) (Fig. 3A to C and Fig. S6). Half-maximum binding titer (EC_{50}) ranged from 0.66 to 1.2 $\mu\text{g}/\text{mL}$ for PGM and 0.57 to 1.2 $\mu\text{g}/\text{mL}$ for B saliva. Den Haag 2017 bound to B saliva as described for the other GII.4 VLPs (EC_{50} , 1.4 $\mu\text{g}/\text{mL}$) but bound only weakly to PGM (EC_{50} , $>8 \mu\text{g}/\text{mL}$). Den Haag 2017-PGM binding could be partially compensated by inclusion of bile (EC_{50} , 3.7 $\mu\text{g}/\text{mL}$), a norovirus ligand binding and cellular infection cofactor (Fig. 3C and Fig. S6) (35–37). Retention of binding to B antigen is likely mediated by 393N as this residue has been previously shown to stabilize GII.4 binding to B antigen (8), although residues in antigenic site A may also contribute to HBGA binding affinity. No other tested GII.4 variants required bile for binding

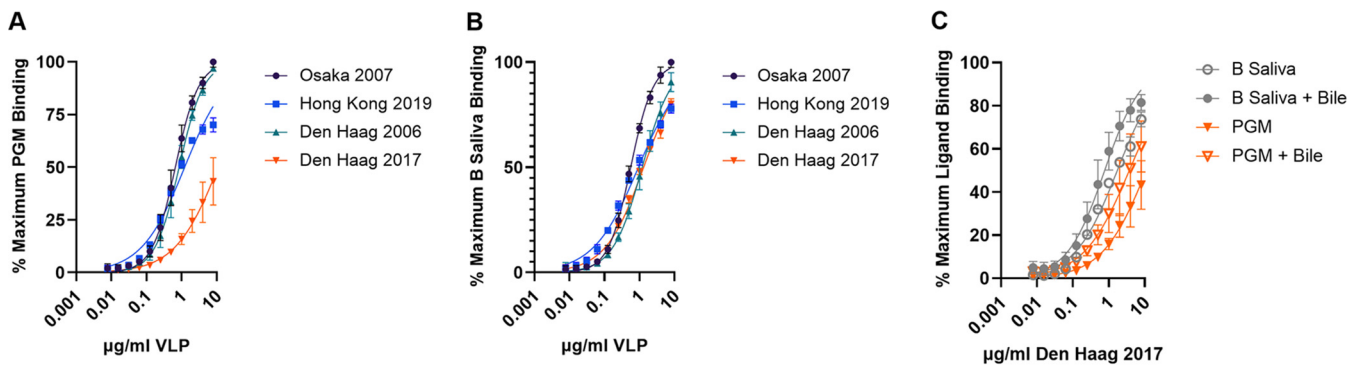


FIG 3 Impact of GII.4 variant evolution on ligand binding. GII.4 Osaka 2007, Hong Kong 2019, and Den Haag 2006 have typical GII.4 ligand binding patterns interacting with PGM (A) and B-type salivary ligands (B). Den Haag 2017 has lower avidity for PGM than but similar avidity for B-type saliva as the other GII.4 variants. Addition of bile stabilizes binding of Den Haag 2017 to ligands (C). Maximum binding was defined by Osaka 2007. Markers denote the mean and standard deviation from two replicates tested in two independent experiments.

to PGM, indicating sufficient avidity for ligand interaction without cofactors (Fig. S6) (35). The dependence of Den Haag 2017 on bile for sufficient avidity potentially indicates that residue changes in Den Haag 2017 might be deleterious to viral fitness compared to other GII.4 variants. In contrast, Hong Kong 2019 interaction with cellular ligands was similar to that of other GII.4 variants (Fig. 3A and B). Inclusion of ligand binding characteristics suggests that the global outbreak potential of Den Haag 2017 viruses is relatively diminished while the potential for Hong Kong 2019 is maintained, based on avidity for the diverse sampling of cellular binding ligands found in the human population.

Evaluation of divergent variant emergence potential based on population serum antibody reactivity. Among individuals genetically susceptible to GII.4 infection (those who express ABO antigens on mucosal surfaces), human norovirus GII.4 global outbreak potential depends on the presence of key residues in neutralizing Ab (NAb) antigenic sites that allow the virus to escape prevailing population immunity (7, 8, 25, 27, 38, 39). Here, we evaluated the antigenicity of Den Haag 2017 and Hong Kong 2019 in the context of prevalent population immunity at the peak of Sydney 2012 circulation in the United Kingdom in 2013 to 2014 (40) (Fig. 4), by measuring the potency of blockade of ligand binding in a surrogate neutralization assay. Sera were collected from young children (1 to 2 years) and healthy adults (≥ 15 years) in 2013 to 2014 and in 2012 to 2014, respectively (41). Individual infection history is unknown, but norovirus is the leading cause of gastroenteritis in the United Kingdom (42). To exclude samples from individuals potentially genetically resistant to GII.4 infection, only sera with a GII.4 Sydney blockade antibody titer of ≥ 40 were included in the analyses (young children, $n = 34$; healthy adults, $n = 25$). Although cross-sectional samples are unable to capture changes in an individual's response over time, population patterns of responses may be observed for sets of sera.

Among children sampled in 2013 to 2014, the blockade potencies for Den Haag 2006, Osaka 2007, and Sydney 2012 were similar (geometric mean titer [GMT] range, 679 to 811) (Fig. 4A), even though these children had likely been predominantly, although not exclusively, exposed to Sydney 2012, based on child age and year of sample collection. In comparison, the blockade potencies against the newly observed Den Haag 2017 and Hong Kong 2019 variants by children's sera were substantially lower, by 2- and 9-fold, respectively, than those against Sydney 2012. Despite being collected at the height of Sydney 2012 predominance, the adult sera from 2012 to 2014 had the strongest blockade potency against Den Haag 2006 (GMT, 825) and Osaka 2007 (GMT, 798), with Sydney 2012 lower by 3-fold (Fig. 4B). The blockade of Den Haag 2017 was 2-fold lower, similar to that observed with the children's sera, while blockade of Hong Kong 2019 was 5-fold lower.

To evaluate these findings in the context of more contemporary population immunity, we made the same comparison with sera collected from healthy adults in 2017 to 2019 ($n = 19$) (Fig. 4C) and young children with a confirmed first GII.4 infection

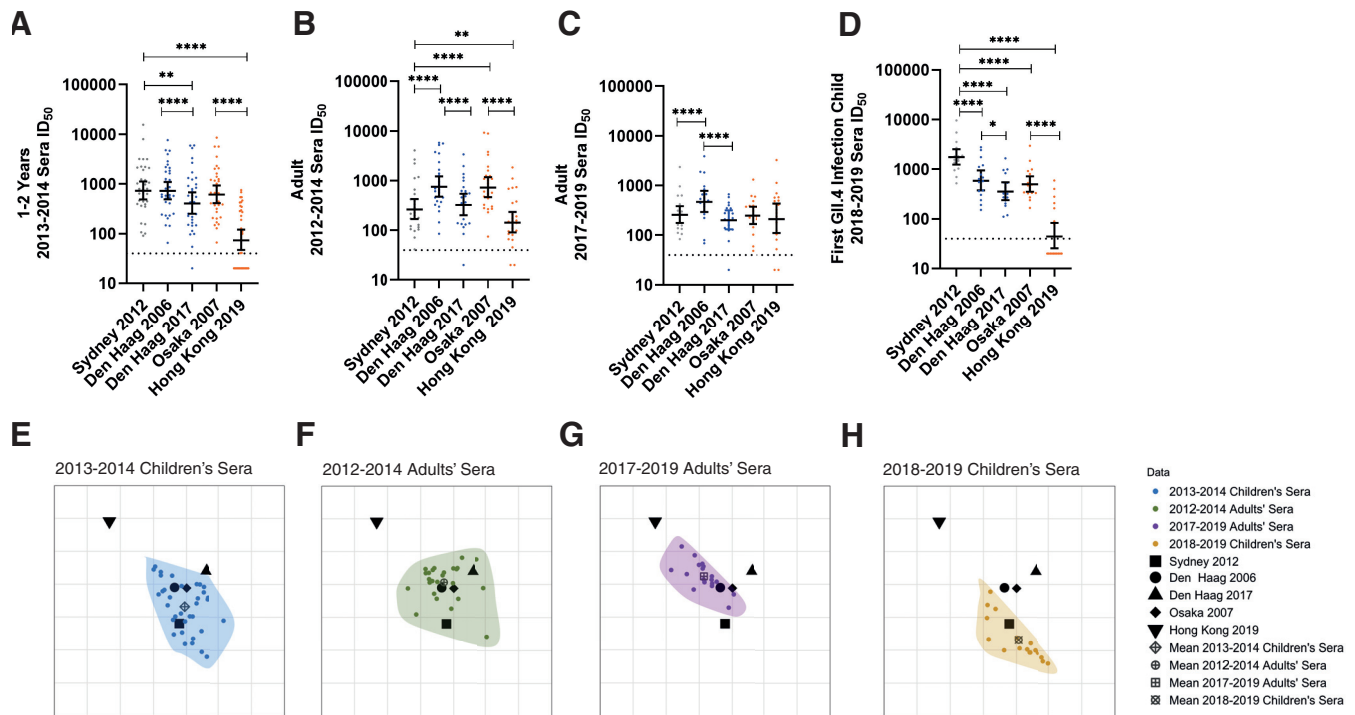


FIG 4 Antigenic divergence of novel strains depends on exposure history of the population. (A to D) Blockade antibody titer in sera from children aged 1 to 2 years in 2013 to 2014 ($n = 34$) (A), adults in 2012 to 2014 ($n = 25$) (B), adults in 2017 to 2019 ($n = 19$) (C), and children ($n = 17$) after their first GII.4 (Sydney 2012) infection in 2018 to 2019 (D). Marker, individual response. Line, geometric mean titer. Error bars, 95% confidence intervals. *, $P \leq 0.03$; **, $P \leq 0.0021$; ****, $P < 0.0001$, Wilcoxon matched-pairs signed-rank test, compared to Sydney 2012 or between the two Den Haag VLPs or Osaka 2007 and Hong Kong 2019. (E to H) Antigenic cartography analysis across all serum sets, divided into separate panels for clarity: children in 2013 to 2014 (E), adults in 2012 to 2014 (F), adults in 2017 to 2019 (G), and children in 2018 to 2019 (H). Virus variants are represented as distinct black shapes, and each serological data set is represented by distinct colors and with data points encapsulated in a shaded polygon. The mean of the serological points for each serum set is indicated by distinct dark gray shapes. One grid box corresponds to a 2-fold change in titer. Note that the orientation of the plots does not matter.

sequence verified as Sydney 2012 (median age, 12 months [interquartile range {IQR}, 7 to 13 months], $n = 17$) (Fig. 4D). As shown for adult sera in 2012 to 2014, blockade antibody potency among adults in 2017 to 2019 was skewed toward Den Haag 2006, 2-fold higher than that against Sydney 2012. In addition, blockade titers were not statistically significantly different between Sydney 2012, Den Haag 2017, Osaka 2007, and Hong Kong 2019 (GMT range, 214 to 271; Wilcoxon $P > 0.05$). Titer to Den Haag 2006 was not statistically significantly different between the 2012–2014 and 2017–2019 adult serum sets (Mann-Whitney $P = 0.23$). In comparison, titers in sera collected from children recently experiencing their first GII.4 infection with Sydney 2012 in 2018 to 2019 were highly skewed toward Sydney 2012 (GMT, 1,810) with decreased titers to Den Haag 2006 (3-fold), Den Haag 2017 (5-fold), Osaka 2007 (4-fold), and Hong Kong 2019 (35-fold). These data support back-boosting of antibody responses to previous GII.4 variants after Sydney 2012 infection in adults with previous GII.4 exposure.

The breadth of antigenic divergence of the novel variants depends upon the exposure history of the population. To better understand and quantify the antigenic relationships between the GII.4 variants over time and between sets of sera, we used antigenic cartography to visualize the antigen distance (AD) of the viruses to each other compared to each serum set (43–45). One AD equals a 2-fold change in blockade antibody response. A 4-fold change is associated with GII.4 norovirus immune escape in immunized mice (9, 46). We performed a combined analysis including all four sets of sera and all 5 variants. Figure 4E to H shows the antigenic relationships where we have illustrated each serum set separately for visual clarity. The serum sets are shown together in Fig. S7A. Representation of the data in two dimensions (2D) recapitulated the distance matrix generated from 50% inhibitory dilution (ID_{50}) values as well as the

three-dimensional (3D) mapping (Fig. S8A, $R^2 = 0.70$ and 0.73 , respectively). All antigenic distances are reported to the nearest integer. For clarity, we discuss the mean AD for each serum set relative to the variants.

The sera collected from children in 2018 to 2019 clusters most closely with Sydney 2012, with an antigenic distance of 1 between the mean for the sera and Sydney 2012. This is consistent with Sydney 2012 being the first and only GII.4 exposure among these children. In contrast, the sera collected from children in 2013 to 2014 are distributed around Sydney 2012, Den Haag 2006, and Osaka 2007 and close to Den Haag 2017 (all ADs to mean for the sera are 1), indicating children with multiple GII.4 infections develop blockade antibody responses with more breadth than those of singly GII.4-infected children. A similar trend is observed in sera collected from adults in 2012 to 2014, where the sera are clustered around Den Haag 2006 and Osaka 2007, which are closest to the mean (AD to mean for sera of 0), with substantial overlap with Den Haag 2017 and Sydney 2012, which are equidistant to the mean (AD to the mean for sera of 1). Only the adult sera collected in 2017 to 2019 extend toward all norovirus GII.4 variants, including Hong Kong 2019. While the mean for the adult sera collected in 2017 to 2019 still retains its proximity to Den Haag 2006 and Osaka 2007 variants (AD to the mean for sera of 1), the distance of the mean to the Hong Kong 2019 variant is equal to the distance from Sydney 2012 and Den Haag 2017 (AD to the mean for sera of 2), indicating repeat Sydney exposure may be broadening the GII.4 blockade antibody response overall rather than eliciting Sydney-specific responses.

Together, these findings suggest that in naive individuals, antibodies to Sydney 2012 are highly cross-reactive with the antigenically similar Den Haag 2006 and Osaka 2007, while individuals previously exposed to GII.4 norovirus variants show evidence of Den Haag 2006 and Osaka 2007 boosting. Further exposure to Sydney 2012 in previously GII.4-exposed individuals seems to extend existing cross-reactivity to include divergent new variants, even when there is little likelihood of the individuals having ever been exposed to these new variants. In contrast, primary GII.4 infection sera do not result in broad cross-reactivity and are therefore less likely to protect against divergent new variants.

Repeat GII.4 exposure broadens antibody immunity. Of the four sets of sera compared above, only the children's sera collected between 2018 and 2019 have a known GII.4 norovirus infection history (Sydney 2012 infection within the previous 7 months), and these sera have antibody responses specific to the infecting variant. In the other sets of sera comprising individuals with evidence of previous immunity to GII.4 viruses, it is possible that antibody responses specific to a new infecting variant waned faster than the responses of preexisting antibodies, now boosted by reinfection. This could explain the broad antibody responses we see in these populations. To evaluate this, we compared the blockade antibody titer of convalescent-phase sera collected ~21 days after GII.4 infection to those of a panel of time-ordered GII.4 variants spanning from the first known norovirus variant that spread globally in the mid-1990s (US95/96), through to Sydney 2012 (Fig. 5 and Table S1). Convalescent-phase sera after GII.4 infection between 1988 and 1999 preferentially targeted US95/96 (GMT, 2920) with moderate cross-reactivity to Farmington Hills 2002 (4-fold decrease in GMT) but poor cross-reactivity to Den Haag 2006 (18-fold decrease) and New Orleans 2009 and Sydney 2012 (both 24-fold decrease) (Fig. 5A), indicating infection with the first globally dominant US95/96 GII.4 variant, or related viruses, did not result in broad antibody responses at the peak of titer, in agreement with observations on immunity after primary infection with Sydney 2012.

In contrast, convalescent-phase sera after Den Haag 2006 and Sydney 2012 infection were broadly potent across the time-ordered panel of variants with the GMT varying between 0.7- and 2-fold compared to the Den Haag 2006 or Sydney 2012 GMT (Fig. 5B and C). Den Haag serum blockade antibody titers were most potent for US95/96 (GMT of 3,562) followed by Den Haag 2006 (GMT of 2,557), with reduced cross-reactivity to Farmington Hills 2002 (GMT of 1,939), New Orleans 2009 (GMT of

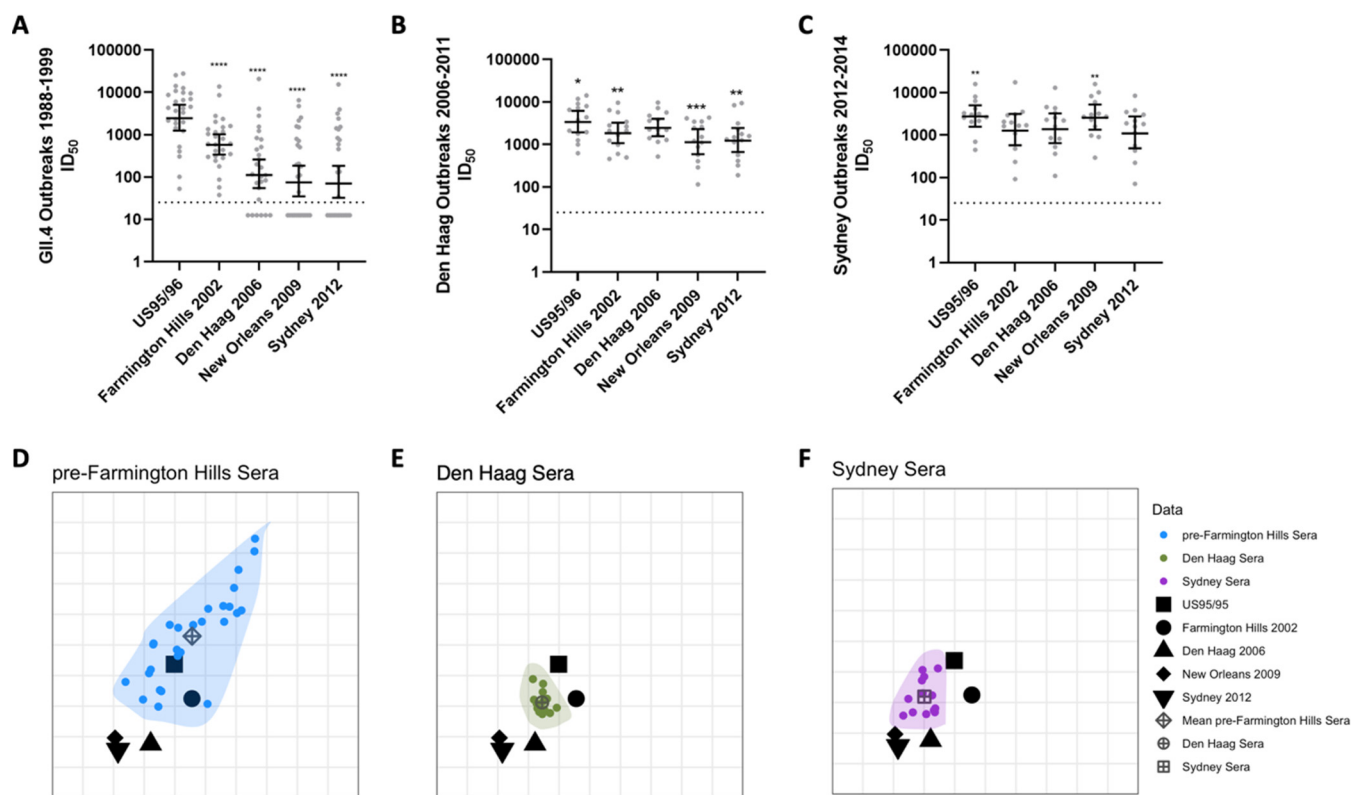


FIG 5 Antigenic divergence measured by convalescent-phase outbreak sera. (A to C) Blockade antibody titer in adult sera collected from GII.4 norovirus outbreaks between 1988 and 1999 ($n = 27$) (A), Den Haag 2006 outbreaks in 2006 to 2011 ($n = 14$) (B), and Sydney outbreaks in 2012 to 2014 ($n = 14$) (C) were compared to time-ordered GII.4 variants. Marker, individual response. Line, geometric mean titer. Error bars, 95% confidence intervals. *, $P \leq 0.03$; **, $P \leq 0.0021$; ***, $P \leq 0.0002$; ****, $P < 0.0001$, Wilcoxon matched-pairs signed-rank test, compared to US95/96 (A), Den Haag 2006 (B), or Sydney 2012 (C). (D to F) Antigenic cartography analysis across all serum sets, divided into separate panels for clarity: pre-Farmington Hills sera (D), Den Haag 2006 sera (E), or Sydney 2012 sera (F). Viral variants are represented as distinct black shapes, and each serological data set is represented by distinct colors and is encapsulated in a shaded polygon. The mean of the serological points for each serum set is indicated by distinct dark gray shapes. One grid box corresponds to a 2-fold change in titer. Note that the orientation of the plots does not matter.

1,227), and Sydney 2012 (GMT of 1,339). Serum titers after Sydney 2012 infection were highest to US95/96 (GMT of 2,899) and New Orleans 2009 (GMT of 2,762) with titers similar to those to Sydney 2012 (GMT of 1,247), Farmington Hills 2002 (GMT of 1,445), and Den Haag 2006 (GMT of 1,536). Thus, convalescent-phase sera collected at the peak of antibody titer indicate that the broad antibody responses characterized in sera from individuals with previous GII.4 exposures are not the result of rapid waning of antibody to the current infecting variant, as individuals infected with Den Haag 2006 or Sydney 2012 also produced maximum titers to noninfecting variants. In all three sets of outbreak sera, GII.4 infection predominantly back-boosted antibodies to US95/96, even when the infecting strain was significantly different. Further, in none of the sets of sera (surveillance or GII.4 outbreaks) likely to have experienced multiple GII.4 infections based on age and variant circulation was the antibody response to Sydney 2012 infection driven predominantly by anti-Sydney 2012 specific antibodies.

As with the surveillance sera, we employed antigenic cartography to better understand and quantify the antigenic relationships between the viral variants relative to the three outbreak sera in 2D (Fig. 5D to F; Fig. S7B). 2D representation recapitulated the distance matrix generated from ID₅₀ values as well as, if not better than, the 3D mapping (Fig. S8B; both $R^2 = 0.65$ and 0.60 , respectively).

The variants cluster into two distinct groups: US95/96 and Farmington Hills 2002, and Den Haag 2006, New Orleans 2009, and Sydney 2012. The antigenic distance between the two clusters (AD range of 2 to 3) is larger than that within each group (AD range of 0 to 1). The antigenic dissimilarity between these two clusters is in line

with the shift in antigenicity that has previously been observed in human sera to coincide with the emergence of the Den Haag 2006 variant (7, 11).

Convalescent-phase sera before Farmington Hills infection cover the largest antigenic space, potentially reflecting the large span of time of sample collection (1988 to 1999), the mean for which is closest to the US95/96 and Farmington Hills 2002 variants (AD of 1 and 2, respectively). In contrast, convalescent-phase sera after Den Haag 2006 infection occupy a much smaller antigenic space, perhaps reflecting the shorter time frame of observation (2006 to 2011). The corresponding mean for these sera is equidistant and closest to strains preceding and including Den Haag 2006 (US95/96, Farmington Hills 2002, Den Haag 2006, AD of 1) and slightly further away from later dominant variants (New Orleans 2009 and Sydney 2012, AD of 2). Similar to convalescent-phase sera after Den Haag 2006 infection, sera after Sydney 2012 infection exhibit a compact distribution. The distribution of these sera retains its proximity to Den Haag 2006 (AD to mean for sera of 1) while broadening in the direction of the other variants (AD to mean of 2) in agreement with trends of back-boosting and broadening of GII.4 antibody responses identified in surveillance sera.

Taken together with the results from nonoutbreak sera, these data illustrate the complexities of population responses, suggesting that population immunity to human norovirus broadens by exposure and is shaped by preexposure histories with back-boosting of previous immunity.

DISCUSSION

Many human norovirus GII.4 variants cocirculate globally without causing increased levels of disease. Global emergence and global predominance of GII.4 noroviruses likely require use of a broad selection of binding ligands with change in a combination of viral characteristics (novel neutralizing epitopes) and host factors (susceptible genetic background and ineffective population immunity). By applying the metrics described here for evaluating the potential for immune evasion and broad host range to viruses selected for sequence divergence, we have established a potential pipeline for predicting the potential of GII.4 human noroviruses to spread globally. Similar approaches may also be applicable to other acute viral infections with cocirculating variants that lack tractable laboratory systems for functional analyses (such as *in vitro* culture). Although both Den Haag 2017 and Hong Kong 2019 have unique residue changes in antigenic sites, the limited number of changes of Den Haag 2017 compared to other Den Haag 2006 strains, its emergence from within the Den Haag 2006 cluster, and its weak interaction with cellular ligands may hinder the potential for Den Haag 2017 to escape from population immunity and efficient transmission. While these data suggest that Hong Kong 2019 is better poised to infect a broad population, to emerge as a dominant variant Hong Kong 2019 would need to evade current population immunity. This variant is able to evade antibody in adult and child sera from 2013 to 2014 and child sera from 2018 to 2019. In contrast, adult sera from 2017 to 2019 contain effective blocking antibodies. This may explain why, although Hong Kong 2019-like strains have occasionally been detected in Asia and Europe, including the United Kingdom, they have failed to increase in numbers. Den Haag 2017 is more effectively blocked by all sera, which may explain why we find no evidence of any similar sequences among our own collection or in any public database.

Understanding the host and virologic factors that facilitate the transition of a GII.4 variant from causing low-level disease in children/asymptomatic infection in adults to a variant that spreads globally, causing symptomatic disease in adults, would increase the reliability of predicting which variants will spread globally and inform vaccine development. GII.4 variants cocirculate and evolve for years, specifically in children (15–17), and it is host factors that appear to be the major driving force that discriminates between variants that cause endemic disease versus those that spread globally. Adults likely become susceptible to symptomatic infection when either antibody neutralization titers wane at mucosal sites or infection reshapes the serological repertoire of

circulating neutralizing/blockade antibodies and provides an avenue for the emergence of a preexisting, epitope-divergent variant with good fitness. Thus, GII.4 variant threat prioritization lists will vary over time and depend on immunity in adults with extensive preexposure history and back-boosted memory antibody responses to human norovirus.

Analyzing sera from exposed and recently infected children and adults demonstrates the complex immune profile that develops from single and sequential exposures to norovirus GII.4 variants. Following the first GII.4 infection, blockade antibody responses demonstrated more specificity to the infecting variant with limited cross-reactivity to other variants, even closely related variants. Subsequent GII.4 variant infection, as has likely occurred in the children and adults sampled in 2013 to 2014, broadened the antibody response to closely related variants (Den Haag 2006 and Osaka 2007) but not the more distant variant (Hong Kong 2019). Finally, repeat exposure to the Sydney 2012 variant over the past decade, based on known variant prevalence data, further broadened the antibody response to include more distant variants such as Hong Kong 2019 in adults sampled in 2017 to 2019. This antibody broadening was replicated within an additional set of commercial adult sera collected in 2019 and correlated with targeting of antigenic site G (41). In adults with a history of exposure to prior GII.4 variants, immunological back-boosting resulted in a mismatch between the current variant and the resulting immune response. For both adult surveillance serum data sets, blockade antibody titers to the Den Haag 2006 variant are higher than those to the Sydney 2012 variant. Taken together, these data suggest that exposure to Sydney 2012 over time results in a broadening of the immune response rather than a recalibrating of the immune response to preferentially neutralize Sydney 2012. Alternatively, there may be key residue changes in 2012 Sydney that induce highly cross-reactive antibody responses, potentially through conformational changes as been described for HIV (47, 48), influenza virus (49), and norovirus and SARS-CoV-2 (50). This widening of immune breadth, and subsequent narrowing of available antigenic space, may explain the lack of a novel dominant variant to yet replace Sydney 2012. Subsequently, waning of population immunity resulting either in lower titer or in reshaping of the serological repertoire by selective loss of specific antibodies, as may have occurred during COVID-19-related behavior modifications, may allow a new variant to emerge.

Supporting these conclusions, using antigenic cartography to compare the relationships between each of the population serum sets and viruses indicates that the breadth of viruses that are neutralized changes over time. Adult sera from 2012 to 2014 and 2017 to 2019 cluster most closely with the Den Haag 2006 and Osaka 2007 viruses, despite continued exposure to Sydney 2012 in the latter group. However, the breadth of viruses neutralized by adult sera from 2017 to 2019 is greater, as evidenced by the proximity of the sera and all variants analyzed. In contrast, child sera from 2012 to 2013 and from 2018 to 2019 both clustered closer to Sydney 2012, the likely most recent infecting strain. However, child sera from 2012 to 2013, with potentially multiple different GII.4 exposures, were more evenly distributed across the variants than child sera from 2018 to 2019 following a single primary exposure. Similar patterns of antigenic breadth were observed with outbreak sera soon after known GII.4 variant infection. Taken together, one interpretation is that the antibody response to Sydney 2012 in adults drives strong GII.4 memory B cell responses to Den Haag 2006. Strong memory B cell responses to Den Haag 2006 could, in turn, reduce antibody responses to Sydney 2012, reflected in the comparably longer mean antigenic distances. This hypothesis is in line with previous findings that GII.4 human norovirus antibody responses in adults postvaccination are primarily memory responses to ancestral GII.4 variants (26, 51). Moreover, human monoclonal antibodies and human polyclonal sera indicate Den Haag 2006 and Sydney 2012 (as well as New Orleans 2009) are antigenically more similar to each other than to previous variants (7, 28, 52). Notably, independent serological and cartographic analyses of GII.4 outbreak sera with known exposure history verify the pattern of broadening immunity and back boosting described in surveillance sera, suggesting that the above observations do not result from selective waning of antibody

responses postinfection but instead reflect the complex dynamics of changing population immunity to human norovirus.

Young children should be the primary target for norovirus vaccination if the aim is to prevent infection and decrease burden of disease (53–55). To be most effective, infants with limited GII.4 exposure will need to be immunized. Here, we show that sera from children are less cross-reactive than sera from adults, particularly following a first GII.4 infection. This finding fits with data showing that younger infants and single-variant-immunized mice have been shown to respond primarily to the infecting variant (9, 46, 56, 57). Greater breadth of immunity likely develops over time as a consequence of multiple infections. How the order or frequency of these infections impacts antibody responses and subsequently serologic and mucosal immunity is unknown but will affect the cross-protection patterns and vaccine formulation requirements as new variants emerge and population immunity shifts. The correlation between serological and mucosal immunity for norovirus and the impact of each on protection against infection and disease is not well studied, especially considering the disease burden.

Incorporating population immunity into a conceptual model of GII.4 variant global emergence likely improves the accuracy of the results but also has challenges. Accurate prediction will require the establishment of a large panel of reagents for the testing pipeline, which is especially complex within the context of continually evolving population immunity and necessitates a continued requirement for contemporary human samples or complex immunization schemes for animals. Here, we assembled a unique resource of sera comprised of both year-matched archived and year-matched contemporary sera. However, we were unable to match the serum sets demographically. Specifically, the first GII.4 infection child sera were collected in a low- to middle-income country with less genetic diversity than the source of the other sera, the United Kingdom and United States. While these features likely impact the likelihood of GII.4 exposure or infection for a child, they are unlikely to directly explain the differences in serum breadth discussed here, as only individuals with serological evidence of GII.4 infection (genetically susceptible) were included in the analyses and the first infection breadth of blockade antibody responses in the children is similar to those reported after single GII.4 immunization of animals and those seen in adults after ancestral GII.4 infection (8, 27).

It also remains uncertain for how long variants might circulate before emergence. It is likely that regular and repeat modeling of adult and child sera will be necessary to differentiate between antibody cross-reactivity and preexposure with defined molecular diagnostics techniques. The roles that adult parents of young children play in accelerating or mitigating transitions of new emergent variants to global outbreaks will also need to be defined. Further, we cannot exclude at this time the possibility that the increase in the numbers of children in the population who are susceptible to a particular GII.4 variant (e.g., Hong Kong 2019), relative to adults with immunity, may itself increase the chance of a global spread of a variant. How these factors interplay with the fact that children initially exposed to Sydney 2012 will have different antibody set points for back-boosting and cross-reactivity has yet to be determined but will guide both the spread of new GII.4 variants and vaccine component requirements in the future. Several of these issues could be addressed by implementing national surveillance systems not only for outbreaks but also for sporadic norovirus cases as well as environmental samples that may better reflect the diversity of infection. These questions apply not only to human norovirus but also to other RNA viruses under selective pressure.

The physical isolation brought on by the COVID-19 pandemic has decreased hospitalizations for influenza, respiratory syncytial virus (RSV), rotavirus, and norovirus infections (58). Norovirus reports decreased by an estimated 40 to 79% during the COVID-19 pandemic (59–61). These stark declines support the potential effectiveness of nonpharmaceutical interventions at controlling norovirus transmission and emphasize the impact that effective surveillance and control measures (e.g., alert systems linked to public health messaging) could have in the absence of a licensed vaccine. Fewer human norovirus infections

during the COVID-19 pandemic imply that population-wide antibody titers have likely waned, potentially setting the stage for emergence of a new GII.4 variant (62).

MATERIALS AND METHODS

Variant data set. Nine hundred thirty GII.4 norovirus samples, with full metadata, collected and sequenced as part of the NoroPatrol Surveillance Project were analyzed here.

Fecal sample collection. Fecal specimens from norovirus RNA-positive patients were referred from outbreak events detected by local and regional National Health Service (NHS) and Public Health England (PHE) laboratories to the National Enteric Virus Reference Laboratory at PHE Colindale. All samples were confirmed norovirus RNA positive by real-time reverse transcription-PCR (RT-PCR) (63) and genotyped by partial capsid sequencing, targeting either region C (64) or the hypervariable P2 domain (65) in open reading frame 2 (ORF2) of the norovirus genome, in accordance with local standard operating procedures.

Fecal specimens were prepared as 10% (wt/vol) suspensions in balanced salt solution (minimal essential medium; Life Technologies), and viral RNA was purified from the supernatants of clarified suspensions using the QIAasympphony, operating the Complex200_v4 protocol with the DSP virus/pathogen kit (Qiagen), eluting RNA in a final volume of 60 μ L. Quantity of norovirus RNA in each sample was estimated by real-time RT-PCR to establish a cycle threshold (C_T) value, and samples with a C_T value of <35 were selected for whole-genome sequencing.

Library preparation and whole-genome sequencing. SuperScript IV (Life Technologies) was used to synthesize single-stranded cDNA from RNA samples. This was followed immediately by second-strand synthesis using the NEBNext mRNA second-strand synthesis module (New England Biolabs) to generate double-stranded cDNA which was purified using AMPure XP magnetic beads (Beckman Coulter). Libraries were prepared using the SureSelect XT low-input reagent kit (Agilent). Briefly, the cDNA was sheared into fragments of ~300 bp using the E220 focused ultrasonicator (Covaris), after which ends were repaired, adenosine tails were added, and adapters were ligated. Adapter-ligated libraries were amplified, incorporating a unique index into each library to allow multiplexed pooling. Libraries were then hybridized with custom-designed biotinylated norovirus RNA baits, and baits were captured using streptavidin-coated magnetic beads. After a second amplification step, the final libraries were quantified, pooled in equimolar amounts, and sequenced on a MiSeq sequencer (Illumina) using a V2 500-cycle kit for 250-bp paired-end reads.

Mapping. Raw read data in paired-end Fastq files were first adapter trimmed, followed by removal of low-quality (<Q30) reads. The reads that passed quality control were then mapped to a large custom data set of norovirus genotype references. From the multimapping BAM file we selected the best reference for the data set based on the number of reads mapping to it and the completeness of the genome. In cases of mixed infection, multiple top references were selected. The reads were then remapped to the best reference or the best set of references (in cases of mixed infection), duplicate reads were removed, and then consensus sequence was called at a minimum depth of 10 reads. Complete analysis was carried out using CLC Genomics Workbench v 11.01. The consensus sequences (Fasta format) are then genotyped using the norovirus genotyping tool hosted at <https://www.rivm.nl/mpf/typingtool/norovirus/>.

Phylogenetic analysis. The maximum likelihood tree of the alignment was constructed using RAxML (66) with the GTR model and 750 bootstrap replicates. The temporal signal of the data set was explored using TempEst (67). The optimum tree root was identified by maximizing the R squared correlation coefficient. Trees were visualized using ggtree (68–70). VP1 amino acid sequences of Den Haag 2006/Den Haag 2017 and Osaka 2007/Hong Kong 2019 were aligned in Geneious Prime 2021.2.2 using the Geneious Alignment tool with default settings.

Serum samples. Sera collected in the United Kingdom were obtained from two sources: sera from children 1 to 2 and 15 years of age were obtained from the Public Health England Seroepidemiology Unit (PHE SEU), and sera from adults collected in the 2012–2014 FluWatch were obtained from the Health Survey for England Biobank (41). The use of coded serum samples was approved by the National Health Service Research Ethics Committee (reference 17/EE/0269), London School of Hygiene and Tropical Medicine (reference LEO12196), University of North Carolina at Chapel Hill (18-0214), and CDC (IRB no. 5051). Sera collected in 2017 to 2019 from adults were purchased from BioIVT (Hicksville, NY). Sera were obtained from a birth cohort study in León, Nicaragua, following the subjects' first reverse transcription-quantitative PCR (RT-qPCR)-confirmed symptomatic Sydney 2012 infection. The study was approved by the Institutional Review Boards of the National Autonomous University of Nicaragua, León (UNAN-León, Acta Number 45, 2017) and the University of North Carolina at Chapel Hill (study number 16-2079). Children experiencing their first GII.4 infection were a median of 12 months old (IQR, 7 to 13 months), and the convalescent-phase sera were collected less than 7 months after GII.4 infection. Outbreak sera were selected from GII.4 outbreaks between 1988 and 2014 based on year and norovirus strain. Convalescent-phase sera were selected from norovirus RT-qPCR-confirmed cases. The epidemiological and demographic data available are summarized in Table S1 in the supplemental material. All sera were received coded with no link back to donor identification and were heat inactivated for 30 min at 56°C before use.

Structural homology modeling. Blockade/neutralizing antibody antigenic sites were mapped onto the surface of Sydney 2012 P domain dimer (PDB 4wzt) and with the PyMOL Molecular Graphics System, version 2.0 (Schrödinger, LLC).

VLP production. Virus-like-particle (VLP)-matched strain accession numbers are in Table S2.

ORF2 genes of all strains except Sydney 2012 (MZ376651) were synthesized by Bio Basic Inc. (Amherst, NY) and inserted directly into the Venezuelan equine encephalitis virus replicon vector for

production of VLPs in baby hamster kidney cells (ATCC CCL-10) as described previously (71, 72). Sydney 2012 (MZ376651) VLPs were produced from baculovirus vectors as described previously (10). VLP particle integrity was verified by ligand and antibody binding and visualization of ~40-nm particles by electron microscopy.

VLP-ligand binding assays. VLPs bound to pig gastric mucin type III (PGM; 10 μ g/mL) (Sigma-Aldrich) or human type B saliva were detected by rabbit polyclonal antiserum (Cocalico Biologicals, Stevens, PA), as described previously (39, 73). If included, 1% bovine bile salts (Sigma-Aldrich) were diluted in phosphate-buffered saline (PBS), aliquoted, and stored at -20°C until use (35, 36).

Blockade of VLP-ligand binding assays. Ligand binding blockade antibody assays were performed as described previously (73, 74). VLPs were pretreated with decreasing concentrations of sera for 1 h and then transferred to ligand-coated plates for 1 h, and bound VLPs were detected as for ligand binding assays. PGM (10 μ g/mL) was the ligand source for the Den Haag 2006, Osaka 2007, and Hong Kong 2019 assays. B saliva supplemented with 1% bile was the ligand source for the Den Haag 2017 assay (35, 36). The percent control binding was compared to that for no serum pretreatment. Mean 50% inhibitory dilution (ID_{50}) titers and 95% confidence intervals (95% CIs) were determined from log(inhibitor) versus normalized response-variable slope curve fit in GraphPad Prism 9.1.2 (26, 51). Sera that did not block at least 50% of VLP binding to ligand at the lowest dilution tested were assigned a titer equal to 0.5 times the lowest tested dilution for statistical analysis.

Antigenic cartography. All ID_{50} titer measurements were used in the process of antigenic cartography. The antigenic map in 2D and 3D was made with Racmac software implemented in RStudio, which implements the methodology as in reference 43. Shaded polygons are defined using function `geom_encircle` (<https://CRAN.R-project.org/package=ggalt>). The data visualizations were created using tidyverse, ggplot2, ggalt, and ggforce packages (<https://CRAN.R-project.org/package=ggalt>, <https://ggplot2.tidyverse.org/>).

Statistical analysis. Blockade antibody titer and ligand binding statistical analyses were performed using GraphPad Prism 9.1.2 (7, 26). ID_{50} values were determined by nonlinear curve fit of normalized data with variable slope (7, 26). ID_{50} values were log transformed for analysis and compared by Wilcoxon matched-pairs signed-rank test when comparing VLPs for a serum set or by Mann-Whitney test when comparing serum sets for the same VLP. Ligand binding data were fit with log(inhibitor) versus response-variable slope (four parameters) for EC_{50} calculation or maximum binding and dissociation constants by single-site binding curve analysis in GraphPad Prism 9.1.2 (75). A difference was considered significant if P was <0.05 .

Data availability. The sequence of Den Haag 2017 and Hong Kong 2019 are available on GenBank with accession codes [OK376714.1](https://www.ncbi.nlm.nih.gov/nuclseq/OK376714.1) and [MT742777.1](https://www.ncbi.nlm.nih.gov/nuclseq/MT742777.1) respectively. ID_{50} values, coordinates in antigenic space and code used to generate figures are available on GitHub (<https://github.com/ftettamanti/norovirus-antigenic-cartography>).

SUPPLEMENTAL MATERIAL

Supplemental material is available online only.

FIG S1, PDF file, 0.1 MB.

FIG S2, PDF file, 0.1 MB.

FIG S3, PDF file, 0.1 MB.

FIG S4, PDF file, 0.1 MB.

FIG S5, PDF file, 0.1 MB.

FIG S6, TIF file, 0.5 MB.

FIG S7, PDF file, 0.1 MB.

FIG S8, PDF file, 0.3 MB.

TABLE S1, PDF file, 0.1 MB.

TABLE S2, PDF file, 0.07 MB.

ACKNOWLEDGMENTS

We thank the Microscopy Services Laboratory, Department of Pathology and Laboratory Medicine, University of North Carolina Chapel Hill, and Shilpi Sheth, LSHTM, for her support of the genomics work through retrieval of specimens and preparation and testing of nucleic acid extracts.

The findings and conclusions in this article are those of the authors and do not necessarily represent the official position of the Centers for Disease Control and Prevention. The funders had no role in study design, data collection and interpretation, or the decision to submit the work for publication.

Funding was provided by the Wellcome Trust [203268/Z/16/Z], and the National Institute of Allergy and Infectious Disease R01 AI148260 and R01AI127845.

The overall design of the study was by R.S.B., J.B., R.A.G., L.C.L., and F.A.T.B. L.C.L., F.A.T.B., P.D.B.-J., S.R., M.L.M., M.Z., S.R.M., H.C., K.M.O., D.K., R.W., H.J.T., and D.J.A. prepared and tested samples, performed experiments, and analyzed results. C.C.C. and

S.B. provided PHE fecal samples for analysis. S.B.D. and F.B. designed and conducted the childhood norovirus studies and provided samples for analysis. V.C. and J.V. designed and conducted the outbreak studies and related sample analysis. The manuscript was primarily written by L.C.L., F.A.T.B., J.B., R.A.G., and R.S.B. with input from all authors.

REFERENCES

- Ahmed SM, Hall AJ, Robinson AE, Verhoef L, Premkumar P, Parashar UD, Koopmans M, Lopman BA. 2014. Global prevalence of norovirus in cases of gastroenteritis: a systematic review and meta-analysis. *Lancet Infect Dis* 14:725–730. [https://doi.org/10.1016/S1473-3099\(14\)70767-4](https://doi.org/10.1016/S1473-3099(14)70767-4).
- Patel MM, Hall AJ, Vinje J, Parashar UD. 2009. Noroviruses: a comprehensive review. *J Clin Virol* 44:1–8. <https://doi.org/10.1016/j.jcv.2008.10.009>.
- Kim L, Liebowitz D, Lin K, Kasperek K, Pasetti MF, Garg SJ, Gottlieb K, Trager G, Tucker SN. 2018. Safety and immunogenicity of an oral tablet norovirus vaccine, a phase I randomized, placebo-controlled trial. *JCI Insight* 3:e121077. <https://doi.org/10.1172/jci.insight.121077>.
- Sherwood J, Mendelman PM, Lloyd E, Liu M, Boslego J, Borkowski A, Jackson A, Faix D, US Navy study team. 2020. Efficacy of an intramuscular bivalent norovirus GII.4 virus-like particle vaccine candidate in healthy US adults. *Vaccine* 38:6442–6449. <https://doi.org/10.1016/j.vaccine.2020.07.069>.
- Lopman BA, Steele D, Kirkwood CD, Parashar UD. 2016. The vast and varied global burden of norovirus: prospects for prevention and control. *PLoS Med* 13:e1001999. <https://doi.org/10.1371/journal.pmed.1001999>.
- Chhabra P, de Graaf M, Parra GI, Chan MC, Green K, Martella V, Wang Q, White PA, Katayama K, Vennema H, Koopmans MPG, Vinjé J. 2019. Updated classification of norovirus genogroups and genotypes. *J Gen Virol* 100:1393–1406. <https://doi.org/10.1099/jgv.0.001318>.
- Lindesmith LC, Beltramello M, Donaldson EF, Corti D, Swanstrom J, Debbink K, Lanzavecchia A, Baric RS. 2012. Immunogenetic mechanisms driving norovirus GII.4 antigenic variation. *PLoS Pathog* 8:e1002705. <https://doi.org/10.1371/journal.ppat.1002705>.
- Lindesmith LC, Donaldson EF, Lobue AD, Cannon JL, Zheng DP, Vinje J, Baric RS. 2008. Mechanisms of GII.4 norovirus persistence in human populations. *PLoS Med* 5:e31. <https://doi.org/10.1371/journal.pmed.0050031>.
- Kendra JA, Tohma K, Ford-Siltz LA, Lepore CJ, Parra GI. 2021. Antigenic cartography reveals complexities of genetic determinants that lead to antigenic differences among pandemic GII.4 noroviruses. *Proc Natl Acad Sci U S A* 118:e2015874118. <https://doi.org/10.1073/pnas.2015874118>.
- Allen DJ, Noad R, Samuel D, Gray JJ, Roy P, Iturriza-Gomara M. 2009. Characterisation of a GII-4 norovirus variant-specific surface-exposed site involved in antibody binding. *Virol J* 6:150. <https://doi.org/10.1186/1743-422X-6-150>.
- Lindesmith LC, Donaldson EF, Baric RS. 2011. Norovirus GII.4 strain antigenic variation. *J Virol* 85:231–242. <https://doi.org/10.1128/JVI.01364-10>.
- Ruis C, Roy S, Brown JR, Allen DJ, Goldstein RA, Breuer J. 2017. The emerging GII.P16-GII.4 Sydney 2012 norovirus lineage is circulating worldwide, arose by late-2014 and contains polymerase changes that may increase virus transmission. *PLoS One* 12:e0179572. <https://doi.org/10.1371/journal.pone.0179572>.
- Cannon JL, Barclay L, Collins NR, Wikswo ME, Castro CJ, Magana LC, Gregoricus N, Marine RL, Chhabra P, Vinje J. 2017. Genetic and epidemiologic trends of norovirus outbreaks in the United States from 2013 to 2016 demonstrated emergence of novel GII.4 recombinant viruses. *J Clin Microbiol* 55:2208–2221. <https://doi.org/10.1128/JCM.00455-17>.
- Tohma K, Lepore CJ, Ford-Siltz LA, Parra GI. 2017. Phylogenetic analyses suggest that factors other than the capsid protein play a role in the epidemic potential of GII.2 norovirus. *mSphere* 2:e00187-17. <https://doi.org/10.1128/mSphereDirect.00187-17>.
- Ruis C, Lindesmith LC, Mallory ML, Brewer-Jensen PD, Bryant JM, Costantini V, Monit C, Vinjé J, Baric RS, Goldstein RA, Breuer J. 2020. Preadaptation of pandemic GII.4 noroviruses in unsampled virus reservoirs years before emergence. *Virus Evol* 6:veaa067. <https://doi.org/10.1093/ve/veaa067>.
- Sdiri-Loulizi K, Ambert-Balay K, Gharbi-Khelifi H, Sakly N, Hassine M, Chouchane S, Guediche MN, Pothier P, Aouni M. 2009. Molecular epidemiology of norovirus gastroenteritis investigated using samples collected from children in Tunisia during a four-year period: detection of the norovirus variant GGII.4 Hunter as early as January 2003. *J Clin Microbiol* 47:421–429. <https://doi.org/10.1128/JCM.01852-08>.
- Sdiri-Loulizi K, Khachou A, Khelifi H, Ayouni S, Elhani D, Ambert-Balay K, Rhim A, Kaplon J, Aouni M, de Rougemont A. 2022. Dynamics of norovirus genotype change and early characterization of variants in children with diarrhea in central Tunisia, 2001–2012. *Arch Virol* 167:99–107. <https://doi.org/10.1007/s00705-021-05290-w>.
- van BEEK J, de Graaf M, Al-Hello H, Allen DJ, Ambert-Balay K, Botteldoorn N, Brytting M, Buesa J, Cabrerizo M, Chan M, Cloak F, Di Bartolo I, Guix S, Hewitt J, Iritani N, Jin M, John R, Lederer I, Mans J, Martella V, Maunula L, McAllister G, Niendorf S, Niesters HG, Podkolzin AT, Poljsak-Prijatelj M, Rasmussen LD, Reuter G, Tuite G, Kroneman A, Vennema H, Koopmans MPG, NoroNet. 2018. Molecular surveillance of norovirus, 2005–16: an epidemiological analysis of data collected from the NoroNet network. *Lancet Infect Dis* 18:545–553. [https://doi.org/10.1016/S1473-3099\(18\)30059-8](https://doi.org/10.1016/S1473-3099(18)30059-8).
- Zakikhany K, Allen DJ, Brown D, Iturriza-Gomara M. 2012. Molecular evolution of GII-4 norovirus strains. *PLoS One* 7:e41625. <https://doi.org/10.1371/journal.pone.0041625>.
- Bok K, Abente EJ, Realpe-Quintero M, Mitra T, Sosnovtsev SV, Kapikian AZ, Green KY. 2009. Evolutionary dynamics of GII.4 noroviruses over a 34-year period. *J Virol* 83:11890–11901. <https://doi.org/10.1128/JVI.00864-09>.
- Sandmann FG, Shallcross L, Adams N, Allen DJ, Coen PG, Jeanes A, Kozlakidis Z, Larkin L, Wurie F, Robotham JV, Jit M, Deeny SR. 2018. Estimating the hospital burden of norovirus-associated gastroenteritis in England and its opportunity costs for nonadmitted patients. *Clin Infect Dis* 67:693–700. <https://doi.org/10.1093/cid/ciy167>.
- Queiros-Reis L, Lopes-João A, Mesquita JR, Penha-Gonçalves C, Nascimento MSJ. 2021. Norovirus gastroenteritis outbreaks in military units: a systematic review. *BMJ Mil Health* 167:59–62. <https://doi.org/10.1136/bmjilitary-2019-001341>.
- Havumaki J, Eisenberg JNS, Mattison CP, Lopman BA, Ortega-Sanchez IR, Hall AJ, Hutton DW, Eisenberg MC. 2021. Immunologic and epidemiologic drivers of norovirus transmission in daycare and school outbreaks. *Epidemiology* 32:351–359. <https://doi.org/10.1097/EDE.0000000000001322>.
- Cannon JL, Bonifacio J, Bucardo F, Buesa J, Bruggink L, Chan MC, Fumian TM, Giri S, Gonzalez MD, Hewitt J, Lin JH, Mans J, Muñoz C, Pan CY, Pang XL, Pietsch C, Rahman M, Sakon N, Selvarangan R, Browne H, Barclay L, Vinjé J. 2021. Global trends in norovirus genotype distribution among children with acute gastroenteritis. *Emerg Infect Dis* 27:1438–1445. <https://doi.org/10.3201/eid2705.204756>.
- Lindesmith LC, McDaniel JR, Changela A, Verardi R, Kerr SA, Costantini V, Brewer-Jensen PD, Mallory ML, Voss WN, Boutz DR, Blazeck JJ, Ippolito GC, Vinje J, Kwong PD, Georgiou G, Baric RS. 2019. Sera Antibody repertoire analyses reveal mechanisms of broad and pandemic strain neutralizing responses after human norovirus vaccination. *Immunity* 50:1530–1541.e8. <https://doi.org/10.1016/j.immuni.2019.05.007>.
- Lindesmith LC, Ferris MT, Mullan CW, Ferreira J, Debbink K, Swanstrom J, Richardson C, Goodwin RR, Baehner F, Mendelman PM, Bargatzke RF, Baric RS. 2015. Broad blockade antibody responses in human volunteers after immunization with a multivalent norovirus VLP candidate vaccine: immunological analyses from a phase I clinical trial. *PLoS Med* 12:e1001807. <https://doi.org/10.1371/journal.pmed.1001807>.
- Cannon JL, Lindesmith LC, Donaldson EF, Saxe L, Baric RS, Vinje J. 2009. Herd immunity to GII.4 noroviruses is supported by outbreak patient sera. *J Virol* 83:5363–5374. <https://doi.org/10.1128/JVI.02518-08>.
- Debbink K, Lindesmith LC, Donaldson EF, Costantini V, Beltramello M, Corti D, Swanstrom J, Lanzavecchia A, Vinje J, Baric RS. 2013. Emergence of new pandemic GII.4 Sydney norovirus strain correlates with escape from herd immunity. *J Infect Dis* 208:1877–1887. <https://doi.org/10.1093/infdis/jit370>.
- Lindesmith L, Moe C, Marionneau S, Ruvoen N, Jiang X, Lindblad L, Stewart P, LePendu J, Baric R. 2003. Human susceptibility and resistance to Norwalk virus infection. *Nat Med* 9:548–553. <https://doi.org/10.1038/nm860>.
- Tan M, Jiang X. 2005. Norovirus and its histo-blood group antigen receptors: an answer to a historical puzzle. *Trends Microbiol* 13:285–293. <https://doi.org/10.1016/j.tim.2005.04.004>.
- Lindesmith LC, Brewer-Jensen PD, Mallory ML, Yount B, Collins MH, Debbink K, Graham RL, Baric RS. 2019. Human norovirus epitope D plasticity allows escape from antibody immunity without loss of capacity for binding cellular ligands. *J Virol* 93:e01813-18. <https://doi.org/10.1128/JVI.01813-18>.

32. de Rougemont A, Ruvoen-Clouet N, Simon B, Estienney M, Elie-Caille C, Aho S, Pothier P, Le Pendu J, Boireau W, Belliot G. 2011. Qualitative and quantitative analysis of the binding of GII.4 norovirus variants onto human blood group antigens. *J Virol* 85:4057–4070. <https://doi.org/10.1128/JVI.02077-10>.
33. Shanker S, Czado R, Sankaran B, Atmar RL, Estes MK, Prasad BV. 2014. Structural analysis of determinants of histo-blood group antigen binding specificity in genogroup I noroviruses. *J Virol* 88:6168–6180. <https://doi.org/10.1128/JVI.00201-14>.
34. Tohma K, Ford-Siltz LA, Kendra JA, Parra GI. 2022. Dynamic immunodominance hierarchy of neutralizing antibody responses to evolving GII.4 noroviruses. *Cell Rep* 39:110689. <https://doi.org/10.1016/j.celrep.2022.110689>.
35. Lindesmith LC, Brewer-Jensen PD, Mallory ML, Jensen K, Yount BL, Costantini V, Collins MH, Edwards CE, Sheahan TP, Vinje J, Baric RS. 2020. Virus-host interactions between nonsecretors and human norovirus. *Cell Mol Gastroenterol Hepatol* 10:245–267. <https://doi.org/10.1016/j.jcmgh.2020.03.006>.
36. Mallory ML, Lindesmith LC, Brewer-Jensen PD, Graham RL, Baric RS. 2020. Bile facilitates human norovirus interactions with diverse histoblood group antigens, compensating for capsid microvariation observed in 2016–2017 GII.2 strains. *Viruses* 12:989. <https://doi.org/10.3390/v12090989>.
37. Tenge VR, Murakami K, Salmen W, Lin SC, Crawford SE, Neill FH, Prasad BVV, Atmar RL, Estes MK. 2021. Bile goes viral. *Viruses* 13:998. <https://doi.org/10.3390/v13060998>.
38. Debbink K, Donaldson EF, Lindesmith LC, Baric RS. 2012. Genetic mapping of a highly variable norovirus GII.4 blockade epitope: potential role in escape from human herd immunity. *J Virol* 86:1214–1226. <https://doi.org/10.1128/JVI.06189-11>.
39. Lindesmith LC, Kocher JF, Donaldson EF, Debbink K, Mallory ML, Swann EW, Brewer-Jensen PD, Baric RS. 2017. Emergence of novel human norovirus GII.17 strains correlates with changes in blockade antibody epitopes. *J Infect Dis* 216:1227–1234. <https://doi.org/10.1093/infdis/jix385>.
40. Allen DJ, Adams NL, Aladin F, Harris JP, Brown DW. 2014. Emergence of the GII-4 norovirus Sydney2012 strain in England, winter 2012–2013. *PLoS One* 9:e88978. <https://doi.org/10.1371/journal.pone.0088978>.
41. Lindesmith LC, Brewer-Jensen PD, Mallory ML, Zweigart MR, May SR, Kelly D, Williams R, Becker-Dreps S, Bucardo F, Allen DJ, Breuer J, Baric RS. 2022. Antigenic site immunodominance redirection following repeat variant exposure. *Viruses* 14:1293. <https://doi.org/10.3390/v14061293>.
42. Harris JP, Iturriza-Gomara M, O'Brien SJ. 2017. Re-assessing the total burden of norovirus circulating in the United Kingdom population. *Vaccine* 35:853–855. <https://doi.org/10.1016/j.vaccine.2017.01.009>.
43. Smith DJ, Lapedes AS, de Jong JC, Bestebroer TM, Rimmelzwaan GF, Osterhaus AD, Fouchier RA. 2004. Mapping the antigenic and genetic evolution of influenza virus. *Science* 305:371–376. <https://doi.org/10.1126/science.1097211>.
44. Wang Y, Tang CY, Wan XF. 2022. Antigenic characterization of influenza and SARS-CoV-2 viruses. *Anal Bioanal Chem* 414:2841–2881. <https://doi.org/10.1007/s00216-021-03806-6>.
45. Chen RE, Smith BK, Errico JM, Gordon DN, Winkler ES, VanBlargan LA, Desai C, Handley SA, Dowd KA, Amaro-Carambot E, Cardoso MJ, Sariol CA, Kallas EG, Sekaly RP, Vasilakis N, Fremont DH, Whitehead SS, Pierson TC, Diamond MS. 2021. Implications of a highly divergent dengue virus strain for cross-neutralization, protection, and vaccine immunity. *Cell Host Microbe* 29:1634–1648.e5. <https://doi.org/10.1016/j.chom.2021.09.006>.
46. Debbink K, Lindesmith LC, Ferris MT, Swanstrom J, Beltramello M, Corti D, Lanzavecchia A, Baric RS. 2014. Within-host evolution results in antigenically distinct GII.4 noroviruses. *J Virol* 88:7244–7255. <https://doi.org/10.1128/JVI.00203-14>.
47. Andrabi R, Su CY, Liang CH, Shivatare SS, Briney B, Voss JE, Nawazi SK, Wu CY, Wong CH, Burton DR. 2017. Glycans function as anchors for antibodies and help drive HIV broadly neutralizing antibody development. *Immunity* 47:524–537.e3. <https://doi.org/10.1016/j.immuni.2017.08.006>.
48. Jain S, Urtsitsky G, Mahalingam M, Batra H, Chand S, Trinh H, Beck C, Shin WH, AlSalami W, Kijak G, Eller LA, Kim J, Kihara D, Tovnanbutra S, Ferrari G, Robb M, Rao M, Rao VB. 2021. A genetic shift in an escaped transmitted/founder virus guides combinatorial vaccine design against HIV-1. *bioRxiv*. <https://doi.org/10.1101/2021.06.16.448593>.
49. Adachi Y, Tonouchi K, Nithichanon A, Kuraoka M, Watanabe A, Shinnakasu R, Asanuma H, Aina A, Ohmi Y, Yamamoto T, Ishii KJ, Hasegawa H, Takeyama H, Lertmemongkolchai G, Kurosaki T, Ato M, Kelsoe G, Takahashi Y. 2019. Exposure of an occluded hemagglutinin epitope drives selection of a class of cross-protective influenza antibodies. *Nat Commun* 10:3883. <https://doi.org/10.1101/2021.06.16.448593>.
50. Jette CA, Cohen AA, Gnanapragasam PNP, Muecksch F, Lee YE, Huey-Tubman KE, Schmidt F, Hatziioannou T, Bieniasz PD, Nussenzweig MC, West AP, Jr, Keeffe JR, Bjorkman PJ, Barnes CO. 2021. Broad cross-reactivity across sarbecoviruses exhibited by a subset of COVID-19 donor-derived neutralizing antibodies. *Cell Rep* 36:109760. <https://doi.org/10.1016/j.celrep.2021.109760>.
51. Lindesmith LC, Mallory ML, Jones TA, Richardson C, Goodwin RR, Baehner F, Mendelman PM, Bargatzke RF, Baric RS. 2017. Impact of pre-exposure history and host genetics on antibody avidity following norovirus vaccination. *J Infect Dis* 215:984–991. <https://doi.org/10.1093/infdis/jix045>.
52. Lindesmith LC, Costantini V, Swanstrom J, Debbink K, Donaldson EF, Vinje J, Baric RS. 2013. Emergence of a norovirus GII.4 strain correlates with changes in evolving blockade epitopes. *J Virol* 87:2803–2813. <https://doi.org/10.1128/JVI.03106-12>.
53. Gaythorpe KAM, Trotter CL, Conlan AJK. 2018. Modelling norovirus transmission and vaccination. *Vaccine* 36:5565–5571. <https://doi.org/10.1016/j.vaccine.2018.07.053>.
54. Steimle LN, Havumaki J, Eisenberg MC, Eisenberg JNS, Prosser LA, Pike J, Ortega-Sanchez IR, Mattison CP, Hall AJ, Steele MK, Lopman BA, Hutton DW. 2021. Cost-effectiveness of pediatric norovirus vaccination in daycare settings. *Vaccine* 39:2133–2145. <https://doi.org/10.1016/j.vaccine.2021.02.066>.
55. Bartsch SM, O'Shea KJ, Wedlock PT, Ferguson MC, Siegmund SS, Lee BY. 2021. Potential clinical and economic value of norovirus vaccination in the community setting. *Am J Prev Med* 60:360–368. <https://doi.org/10.1016/j.amepre.2020.10.022>.
56. Tamminen K, Malm M, Vesikari T, Blazevic V. 2019. Immunological cross-reactivity of an ancestral and the most recent pandemic norovirus GII.4 variant. *Viruses* 11:91. <https://doi.org/10.3390/v11020091>.
57. Blazevic V, Malm M, Honkanen H, Knip M, Hyöty H, Vesikari T. 2016. Development and maturation of norovirus antibodies in childhood. *Microbes Infect* 18:263–269. <https://doi.org/10.1016/j.micinf.2015.12.004>.
58. Fukuda Y, Tsugawa T, Nagaoka Y, Ishii A, Nawa T, Togashi A, Kunizaki J, Hirakawa S, Iida J, Tanaka T, Kizawa T, Yamamoto D, Takeuchi R, Sakai Y, Kikuchi M, Nagai K, Asakura H, Tanaka R, Yoshida M, Hamada R, Kawasaki Y. 2021. Surveillance in hospitalized children with infectious diseases in Japan: pre- and post-coronavirus disease 2019. *J Infect Chemother* 27:1639–1647. <https://doi.org/10.1016/j.jiac.2021.07.024>.
59. Ondrikova N, Clough HE, Douglas A, Iturriza-Gomara M, Larkin L, Vivancos R, Harris JP, Cunliffe NA. 2021. Differential impact of the COVID-19 pandemic on laboratory reporting of norovirus and *Campylobacter* in England: a modelling approach. *PLoS One* 16:e0256638. <https://doi.org/10.1371/journal.pone.0256638>.
60. Ahn SY, Park JY, Lim IS, Chae SA, Yun SW, Lee NM, Kim SY, Choi BS, Yi DY. 2021. Changes in the occurrence of gastrointestinal infections after COVID-19 in Korea. *J Korean Med Sci* 36:e180. <https://doi.org/10.3346/jkms.2021.36.e180>.
61. Douglas A, Sandmann FG, Allen DJ, Celma CC, Beard S, Larkin L. 2021. Impact of COVID-19 on national surveillance of norovirus in England and potential risk of increased disease activity in 2021. *J Hosp Infect* 112:124–126. <https://doi.org/10.1016/j.jhin.2021.03.006>.
62. O'Reilly KM, Sandman F, Allen D, Jarvis CI, Gimma A, Douglas A, Larkin L, Wong KL, Baguelin M, Baric RS, Lindesmith LC, Goldstein RA, Breuer J, Edmunds WJ. 2021. Predicted norovirus resurgence in 2021–2022 due to the relaxation of nonpharmaceutical interventions associated with COVID-19 restrictions in England: a mathematical modelling study. *BMC Med* 19:299. <https://doi.org/10.1186/s12916-021-02153-8>.
63. Kageyama T, Kojima S, Shinohara M, Uchida K, Fukushi S, Hoshino FB, Takeda N, Katayama K. 2003. Broadly reactive and highly sensitive assay for Norwalk-like viruses based on real-time quantitative reverse transcription-PCR. *J Clin Microbiol* 41:1548–1557. <https://doi.org/10.1128/JCM.41.4.1548-1557.2003>.
64. Kojima S, Kageyama T, Fukushi S, Hoshino FB, Shinohara M, Uchida K, Natori K, Takeda N, Katayama K. 2002. Genogroup-specific PCR primers for detection of Norwalk-like viruses. *J Virol Methods* 100:107–114. [https://doi.org/10.1016/s0166-0934\(01\)00404-9](https://doi.org/10.1016/s0166-0934(01)00404-9).
65. Allen DJ, Gray JJ, Gallimore CI, Xerry J, Iturriza-Gomara M. 2008. Analysis of amino acid variation in the P2 domain of the GII-4 norovirus VP1 protein reveals putative variant-specific epitopes. *PLoS One* 3:e1485. <https://doi.org/10.1371/journal.pone.0001485>.
66. Stamatakis A. 2006. RAxML-VI-HPC: maximum likelihood-based phylogenetic analyses with thousands of taxa and mixed models. *Bioinformatics* 22:2688–2690. <https://doi.org/10.1093/bioinformatics/btl446>.
67. Rambaut A, Lam TT, Max Carvalho L, Pybus OG. 2016. Exploring the temporal structure of heterochronous sequences using TempEst (formerly Path-O-Gen). *Virus Evol* 2:vew007. <https://doi.org/10.1093/ve/vew007>.
68. Yu G. 2020. Using ggtree to visualize data on tree-like structures. *Curr Protoc Bioinformatics* 69:e96. <https://doi.org/10.1002/cpbi.96>.

69. Yu G, Lam TT, Zhu H, Guan Y. 2018. Two methods for mapping and visualizing associated data on phylogeny using Ggtree. *Mol Biol Evol* 35: 3041–3043. <https://doi.org/10.1093/molbev/msy194>.
70. Yu G, Smith DK, Zhu H, Guan Y, Tsan-Yuk Lam T. 2017. ggtree: an R package for visualization and annotation of phylogenetic trees with their covariates and other associated data. *Methods Ecol Evol* 8:28–36. <https://doi.org/10.1111/2041-210X.12628>.
71. Agnihothram S, Menachery VD, Yount BL, Jr, Lindesmith LC, Scobey T, Whitmore A, Schafer A, Heise MT, Baric RS. 2018. Development of a broadly accessible Venezuelan equine encephalitis virus replicon particle vaccine platform. *J Virol* 92:e00027-18. <https://doi.org/10.1128/JVI.00027-18>.
72. Debbink K, Costantini V, Swanstrom J, Agnihothram S, Vinje J, Baric R, Lindesmith L. 2013. Human norovirus detection and production, quantification, and storage of virus-like particles. *Curr Protoc Microbiol* 31: 15K.1.1–15K.1.45. <https://doi.org/10.1002/9780471729259.mc15k01s31>.
73. Lindesmith LC, Donaldson EF, Beltramello M, Pintus S, Corti D, Swanstrom J, Debbink K, Jones TA, Lanzavecchia A, Baric RS. 2014. Particle conformation regulates antibody access to a conserved GII.4 norovirus blockade epitope. *J Virol* 88:8826–8842. <https://doi.org/10.1128/JVI.01192-14>.
74. Lindesmith LC, Beltramello M, Swanstrom J, Jones TA, Corti D, Lanzavecchia A, Baric RS. 2015. Serum immunoglobulin A cross-strain blockade of human noroviruses. *Open Forum Infect Dis* 2:ofv084. <https://doi.org/10.1093/ofid/ofv084>.
75. Lindesmith LC, Mallory ML, Debbink K, Donaldson EF, Brewer-Jensen PD, Swann EW, Sheahan TP, Graham RL, Beltramello M, Corti D, Lanzavecchia A, Baric RS. 2018. Conformational occlusion of blockade antibody epitopes, a novel mechanism of GII.4 human norovirus immune evasion. *mSphere* 3:e00518-17. <https://doi.org/10.1128/mSphere.00518-17>.